

# NJC

Accepted Manuscript



This is an *Accepted Manuscript*, which has been through the Royal Society of Chemistry peer review process and has been accepted for publication.

*Accepted Manuscripts* are published online shortly after acceptance, before technical editing, formatting and proof reading. Using this free service, authors can make their results available to the community, in citable form, before we publish the edited article. We will replace this *Accepted Manuscript* with the edited and formatted *Advance Article* as soon as it is available.

You can find more information about *Accepted Manuscripts* in the [Information for Authors](#).

Please note that technical editing may introduce minor changes to the text and/or graphics, which may alter content. The journal's standard [Terms & Conditions](#) and the [Ethical guidelines](#) still apply. In no event shall the Royal Society of Chemistry be held responsible for any errors or omissions in this *Accepted Manuscript* or any consequences arising from the use of any information it contains.

Cite this: DOI: 10.1039/c0xx00000x

www.rsc.org/xxxxxx

## ARTICLE TYPE

**Exploring the Influence of Cationic Skeletons on the Arrangement of Isolated  $\text{BO}_3$  Groups Based on  $\text{RbMgBO}_3$ ,  $\text{CsZn}_4(\text{BO}_3)_3$  and  $\text{Cs}_4\text{Mg}_4(\text{BO}_3)_4$** **Zheng Wang,<sup>a,b</sup> Min Zhang,<sup>\*a</sup> Shilie Pan,<sup>\*a</sup> Zhihua Yang,<sup>\*a</sup> Hui Zhang,<sup>a,b</sup> Bingbing Zhang,<sup>a,b</sup> Ying Wang,<sup>a,b</sup> Jing Kang<sup>a,b</sup> and Xiaoxia Lin<sup>a,b</sup>**<sup>5</sup> Received (in XXX, XXX) Xth XXXXXXXXX 20XX, Accepted Xth XXXXXXXXX 20XX

DOI: 10.1039/b000000x

The structures of three borates with isolated  $\text{BO}_3$  groups,  $\text{RbMgBO}_3$ ,  $\text{CsZn}_4(\text{BO}_3)_3$  and  $\text{Cs}_4\text{Mg}_4(\text{BO}_3)_4$ , are determined from single crystal diffraction data for the first time. The introduction of small cations ( $\text{Mg}^{2+}$  and  $\text{Zn}^{2+}$ ) with strong bonding can prevent the formation of B-O network effectively, and are beneficial to obtain the isolated  $\text{BO}_3$  groups. Moreover, the cationic skeletons composed by small cations significantly affect the arrangement of isolated  $\text{BO}_3$  groups. Thermal analysis, infrared and UV-Vis-NIR diffuse reflectance spectroscopy, and electronic band structure calculations were performed on the reported materials.

## Introduction

Borates have a wide variety of chemistry structures: a boron atom may adopt triangular ( $\text{BO}_3$ ) or tetrahedral ( $\text{BO}_4$ ) oxygen coordinations, both of them can polymerize by sharing corner oxygen atoms to form isolated rings and cages or infinite chains, sheets and networks.<sup>1</sup> In addition, it is also found that many borates have promising technical applications, such as nonlinear optical materials, ferroelectric and piezoelectric materials, luminophors and semiconductors.<sup>2</sup> According to the anionic group theory which was suggested by C. T. Chen<sup>3</sup>, a borate crystal consisting of coplanar and dense  $\text{BO}_3$  groups would possess a relatively large birefringence and second harmonic generation (SHG) coefficients.<sup>4</sup> Hence, how to obtain structures with oriented  $\text{BO}_3$  groups has attracted many researchers' interests. Referenced to the research of P. Becker<sup>5</sup>, isolated  $\text{BO}_3$  groups can exist at the ratio of cation: boron  $> 1$ , which means that it is feasible to obtain borates with isolated  $\text{BO}_3$  groups by increasing the proportion of cations in experiments. Previously, many scientists have made a lot of strategies to align the anionic groups to optimize some properties of materials.<sup>1a, 6, 7</sup> Though we may choose isolated  $\text{BO}_3$  groups to construct new structures, up to now, it is still a challenge to control the arrangement of isolated  $\text{BO}_3$  groups in structure to let them work in concert to give maximum contribution rather than canceling out with each other.<sup>7</sup>

Traditionally, it is widely accepted that B-O anionic group determines the structure of borate compounds because  $\text{BO}_3$  and  $\text{BO}_4$  units may form one-dimensional (1D), two-dimensional (2D) or three-dimensional (3D) framework in melts by corner- or edge-sharing firstly, then cations join in to balance the valence charge.<sup>8</sup> However, for the borates that only containing zero-dimensional (0D, isolated)  $\text{BO}_3$  groups, the cationic skeleton may dominate the crystal structure and affect the arrangement of  $\text{BO}_3$

group because of the neglectable interaction force between isolated  $\text{BO}_3$  groups, especially for the small cations with strong bonding (such as  $\text{Be}^{2+}$ ,  $\text{Mg}^{2+}$ ,  $\text{Zn}^{2+}$ ,  $\text{Cd}^{2+}$  and  $\text{Al}^{3+}$ ).<sup>9</sup> Besides, the highly ionized cations (such as alkalis cations) were introduced to balance valence.

Based on the above points, we explore the Rb/Cs-Mg/Zn-B-O systems, and three compounds  $\text{RbMgBO}_3$  (RMBO),  $\text{CsZn}_4(\text{BO}_3)_3$  (CZBO) and  $\text{Cs}_4\text{Mg}_4(\text{BO}_3)_4$  (CMBO) were synthesized. All of them only contain isolated  $\text{BO}_3$  groups because the introduction of small cations ( $\text{Mg}^{2+}$  and  $\text{Zn}^{2+}$ ) with strong bonding can prevent the formation of B-O network effectively. Moreover, the small cations form different dimensional skeletons (three, two and one dimension, respectively) which influence the arrangement of isolated  $\text{BO}_3$  groups. The RMBO and CZBO compounds were first reported by Kurbatov et al. and Smith et al., respectively, using powder X-ray diffraction (XRD) and refined by the Rietveld method.<sup>10</sup> The small crystals of RMBO, CZBO and CMBO were obtained by high temperature solution method and their structures were solved by single-crystal XRD for the first time. In this paper, the syntheses, crystal structures, thermal and optical properties of RMBO, CZBO and CMBO are presented, and the electronic structure was calculated by the first principles method to further explore the structure–property relationship.

## Experimental Section

### Syntheses

All commercially available chemicals ( $\text{Rb}_2\text{CO}_3$ ,  $\text{Cs}_2\text{CO}_3$  (Xinjiang Research Institute of Nonferrous Metals, 99.5%),  $\text{MgF}_2$ ,  $\text{ZnO}$  and  $\text{H}_3\text{BO}_3$  (Tianjin Hongyan Chemical reagent factory, 99.8%)) are of reagent grade and were used as received. Small single crystals of RMBO, CZBO and CMBO were grown by spontaneous crystallization with the

**Table 1.** Crystal data and structure refinement for RMBO, CZBO and CMBO.

Empirical formula	$\text{RbMgBO}_3$	$\text{CsZn}_4(\text{BO}_3)_3$	$\text{Cs}_4\text{Mg}_4(\text{BO}_3)_4$
Formula weight	168.59	570.82	864.12
Temperature (K)	296(2)	296(2)	296(2)
Crystal system	Cubic	Monoclinic	Monoclinic
Space group, $Z$	$P2_13$ (No. 198), 4	$P2_1/c$ (No. 13), 2	$P2_1/c$ (No. 14), 4
$a$ (Å)	6.942(3)	6.871(7)	20.217(6)
$b$ (Å)	6.942(3)	5.021(5)	4.8790(12)
$c$ (Å)	6.942(3)	12.936(13)	16.682(4)
$\alpha$ (°)	90.000	90.000	90.000
$\beta$ (°)	90.000	92.399(11)	114.296(2)
$\gamma$ (°)	90.000	90.000	90.000
Volume (Å <sup>3</sup> )	334.5(3)	445.9(8)	1499.7(7)
Density (calculated, g/cm <sup>3</sup> )	3.348	4.251	3.827
Absorption coefficient (mm <sup>-1</sup> )	14.791	14.681	9.868
$F(000)$	312	524	1536
Index ranges	$-8 \leq h \leq 9, -8 \leq k \leq 9, -4 \leq l \leq 9$	$-8 \leq h \leq 8, -6 \leq k \leq 6, -16 \leq l \leq 15$	$-15 \leq h \leq 26, -5 \leq k \leq 6, -21 \leq l \leq 21$
Reflections collected / unique	1865 / 261 [ $R(\text{int}) =$	2574 / 1025 [ $R(\text{int}) =$	9239 / 3427 [ $R(\text{int}) = 0.0282$ ]

	0.0393]	0.0260]	
Completeness	100.0 %	98.3 %	99.2 %
Refinement method		Full-matrix least-squares on F <sup>2</sup>	
Data/restraints/parameters	261 / 0 / 20	1025 / 0 / 80	3427 / 12 / 219
Goodness-of-fit on F <sup>2</sup>	1.057	1.331	1.083
Final R indices [F <sub>o</sub> <sup>2</sup> > 2σ(F <sub>o</sub> <sup>2</sup> )] <sup>a</sup>	R <sub>1</sub> = 0.0131, wR <sub>2</sub> = 0.0288	R <sub>1</sub> = 0.0215, wR <sub>2</sub> = 0.0614	R <sub>1</sub> = 0.0227, wR <sub>2</sub> = 0.0518
R indices (all data) <sup>a</sup>	R <sub>1</sub> = 0.0140, wR <sub>2</sub> = 0.0290	R <sub>1</sub> = 0.0243, wR <sub>2</sub> = 0.0825	R <sub>1</sub> = 0.0254, wR <sub>2</sub> = 0.0528
Largest diff. peak and hole (e <sup>-</sup> Å <sup>-3</sup> )	0.238 and -0.208	1.136 and -0.844	1.052 and -1.189

$$^a R1 = \sum |F_o| - |F_c| / \sum |F_o| \text{ and } wR2 = [\sum w(F_o^2 - F_c^2)^2 / \sum wF_o^4]^{1/2} \text{ for } F_o^2 > 2\sigma(F_o^2)$$

same molar ratio of Rb<sub>2</sub>CO<sub>3</sub>: MgF<sub>2</sub>: H<sub>3</sub>BO<sub>3</sub>, Cs<sub>2</sub>CO<sub>3</sub>: ZnO: H<sub>3</sub>BO<sub>3</sub> and Cs<sub>2</sub>CO<sub>3</sub>: MgF<sub>2</sub>: H<sub>3</sub>BO<sub>3</sub> equal to 3.5: 1: 4, respectively. A mixture of Rb<sub>2</sub>CO<sub>3</sub> (5.316 g, 23.02 mmol), MgF<sub>2</sub> (0.606 g, 9.73 mmol) and H<sub>3</sub>BO<sub>3</sub> (1.716 g, 27.75 mmol) for RMBO; a mixture of Cs<sub>2</sub>CO<sub>3</sub> (2.308 g, 7.08 mmol), ZnO (0.164 g, 2.01 mmol) and H<sub>3</sub>BO<sub>3</sub> (0.495 g, 8.01 mmol) for CZBO and a mixture of Cs<sub>2</sub>CO<sub>3</sub> (3.257 g, 10.00 mmol), MgF<sub>2</sub> (0.401 g, 6.44 mmol) and H<sub>3</sub>BO<sub>3</sub> (1.238 g, 20.00 mmol) for CMBO were thoroughly ground. The respective mixtures were then placed in a platinum crucible that was placed into a vertical, programmable-temperature furnace. All of the crucibles were gradually heated to 780 °C and held for 10 h, then slowly cooled down to 500 °C at a rate of 2 °C h<sup>-1</sup>, followed by rapid cooling to room temperature. Colorless crystals of RMBO, CZBO and CMBO were obtained, and separated mechanically from the crucible for the further characterization by single-crystal XRD measurements.

Polycrystalline samples of RMBO and CZBO were synthesized via conventional solid-state reactions. A stoichiometric mixture of Rb<sub>2</sub>CO<sub>3</sub>/Cs<sub>2</sub>CO<sub>3</sub>, MgO/ZnO, and borate acid was initially ground and placed in alumina crucibles, then heated to 720 °C and held for 7 days with 14 times grindings and mixings. However, polycrystalline samples of CMBO were difficult to synthesize by conventional solid-state techniques. Although we tried to prepare it using different ratios of precursor and raw materials, CMBO still cannot be synthesized. Finally we used two-step reactions to obtain the polycrystalline samples of CMBO successfully. The detailed procedure is that stoichiometric mixture of MgO and borate acid was calcined at 1100 °C for 12 hours, then Cs<sub>2</sub>CO<sub>3</sub> was added and the mixture was calcined at 720 °C for 7 days with 14 times grindings and mixings.

Powder XRD data of polycrystalline materials were obtained on a Bruker D2 PHASER diffractometer with Cu Kα radiation (λ = 1.5418 Å) at room temperature. The 2θ range was 10–70° with a step size of 0.02° and a fixed counting time of 1s/step. No impurities were observed. The experimental powder XRD patterns shown are in good agreement with the calculated ones derived from the single-crystal data (Figure S1).

### Single-Crystal X-ray Diffraction

Block crystals of RMBO (0.298 mm × 0.168 mm × 0.150 mm), CZBO (0.211 mm × 0.155 mm × 0.053 mm) and CMBO (0.272 mm × 0.213 mm × 0.157 mm) were used for single-crystal data collection. Data were collected on a Bruker SMART APEX II

CCD diffractometer using monochromatic Mo Kα radiation (λ = 0.71073 Å) at 293(2) K and integrated with the SAINT program.<sup>11</sup> The numerical absorption corrections were carried out using the SADABS program<sup>12</sup> for area detector. All calculations were performed with programs from the SHELXTL crystallographic software package.<sup>13</sup> The structures was solved by direct methods using SHELXS-97,<sup>14</sup> and all of the atoms were refined using full-matrix least-squares techniques with anisotropic thermal parameters and final converged for I > 2σ. The structures were checked for missing symmetry elements with PLATON.<sup>15</sup> The crystal data and structure refinement for RMBO, CZBO and CMBO are presented in Table 1. The final refined atomic positions and isotropic thermal parameters are given in Table S1 in the Supporting Information. The selected bond distances are listed in Table S2 in the Supporting Information.

### Thermal Analysis

The thermal behavior of RMBO, CZBO and CMBO was investigated on thermogravimetry and differential scanning calorimeter (TG-DSC) using a NETZSCH STA 449 F3 simultaneous thermal analyzer. The samples were placed in a Pt crucible and heated at a rate of 5 °C/min in the range of 40–1100 °C under flowing of nitrogen gas.

### Linear Optical Properties Measurements

UV-Vis-NIR diffuse-reflectance data were collected with a SolidSpec-3700DUV spectrophotometer using polytetrafluoroethylene as a reference in the wavelength range from 190 to 2600 nm. Reflectance spectra were converted to absorbance using the Kubelka-Munk function<sup>16</sup>, F(R) = (1 - R)<sup>2</sup>/2R, where R is the reflectance.

### Computational Details

First-principles density functional theory (DFT) electronic structure calculations for the three compounds were performed with the total-energy code CASTEP.<sup>17</sup> The exchange correlation effects were treated with the general gradient approximation (GGA) using the Perdew-Burke-Ernzerhof (PBE) functional.<sup>18</sup> The interactions between the ionic cores and the electrons were described by the ultrasoft pseudopotentials.<sup>19</sup> The Monkhorst-Pack scheme k-point grid sampling was set at 4 × 4 × 4 for RMBO and CMBO and 2 × 3 × 1 for CZBO in the primitive cell of the Brillouin zone (BZ) for the total energy calculations. The plane-wave cutoff energy was set to 380.0 eV, which proved to be an optimal level of the total energy convergence. The

following orbital electrons were treated as valence electrons: (1) RMBO: Rb,  $4p^65s^1$ ; Mg,  $2p^63s^2$ ; B,  $2s^22p^1$ ; and O,  $2s^22p^4$ ; (2) CZBO: Cs,  $5p^66s^1$ ; Zn,  $3p^63d^{10}4s^2$ ; B,  $2s^22p^1$ ; and O,  $2s^22p^4$ ; (3) CMBO: Cs,  $5p^66s^1$ ; Mg,  $2p^63s^2$ ; B,  $2s^22p^1$ ; and O,  $2s^22p^4$ . The other parameters used in the calculations were set by the default values of the CASTEP code.

## Results and Discussion

One noncentrosymmetric compound RMBO and two centrosymmetric compounds CZBO and CMBO have been obtained from Rb/Cs-Mg/Zn-B-O systems. Interestingly, only isolated  $\text{BO}_3$  groups are contained in three compounds. The small crystals and powder samples were acquired by high temperature solution method and traditional solid reaction method, respectively. As follows, we will discuss structures and properties of three compounds.

### Structure of RMBO, CZBO and CMBO

Crystallographic analysis reveals that RMBO belongs to the noncentrosymmetric space group  $P2_13$  (No. 198) with an asymmetric unit consisting of one unique rubidium atom, one unique magnesium atom, one unique boron atom, and three unique oxygen atoms (Table S1 in the Supporting Information). Interestingly, the compound crystallizes in the cubic system, which is quite rare for borates, especially for those containing anisotropic polarized planar  $\text{BO}_3$  groups.<sup>20</sup> In this structure, distorted  $\text{MgO}_6$  octahedra connect into a 3D  $[\text{MgO}_6]_\infty$  framework by corner-sharing (Figure S2a in the Supporting Information). The 3D framework presents two kinds of voids: triangular one occupied by  $\text{BO}_3$  groups and quadrate one occupied by large  $\text{Rb}^+$  cations (Figure 1). The Mg-O bond distances are approximately equal ( $2.118(2)$ – $2.166(2)$  Å), and the B-O distances ( $1.3687(18)$  Å) and O-B-O bond angles ( $119.949(15)^\circ$ ) in  $\text{BO}_3$  triangles are typical and equal. The  $\text{Rb}^+$  cations are coordinated with nine oxygen atoms and Rb-O bond distances range from  $2.850(2)$  to  $3.337(2)$  Å (an average distance of  $3.035$  Å). All of the bond lengths are consistent with those observed in other compounds.<sup>21</sup> The results of bond valence sum calculations (BVS)<sup>22</sup> are consistent with the valences of all elements in RMBO (Table S1 in the Supporting Information).

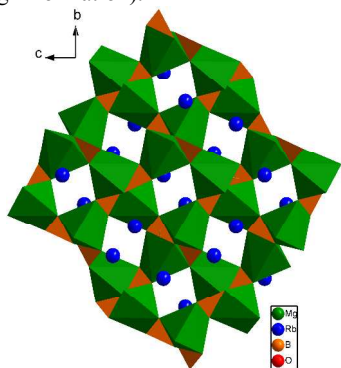


Figure 1. The structure of RMBO.

CZBO crystallizes in the monoclinic space group  $P2_1/c$  (No. 13). One unique cesium atoms, two unique zinc atoms, two unique boron atom, and five unique oxygen atoms are in an asymmetric unit (Table S1 in the Supporting Information). The structure of

CZBO features a 2D infinite  $[\text{Zn}_4\text{O}_9]_\infty$  layer composed of corner-sharing distorted  $\text{ZnO}_4$  tetrahedra with  $\text{B(2)O}_3$  groups inserted into the void space, then adjacent  $[\text{Zn}_4\text{O}_9]_\infty$  layers interconnect into a 3D framework via  $\text{B(1)O}_3$  groups and form a tunnel along  $b$  direction, and  $\text{Cs}^+$  cations reside in the tunnel (Figure 2). The ligands of  $\text{B(1)O}_3$  and  $\text{B(2)O}_3$  groups are quite different in the structure:  $\text{B(2)O}_3$  groups reinforce the 2D Zn-O layer, while the function of  $\text{B(1)O}_3$  groups are connecting the adjacent layers (Figure S2b in the Supporting Information). In the structure, the Zn-O bond lengths range from  $1.906(5)$  to  $1.998(4)$  Å (an average distance of  $1.955$  Å), and the B-O distances are in the range of  $1.345(7)$ – $1.414(7)$  Å (average:  $1.379$  Å). The Zn-O and B-O bond distances are corresponding to that in  $\text{K/RbZn}_4(\text{BO}_3)_3$ .<sup>[10b]</sup> The coordination number of  $\text{Cs}^+$  cations is ten and Cs-O bond distances lie in  $3.121(4)$ – $3.510(4)$  Å (average:  $3.273$  Å). In addition, BVS calculation using Brown's formula for Cs, Zn, B and O also gives reasonable values (Table S1 in the Supporting Information).

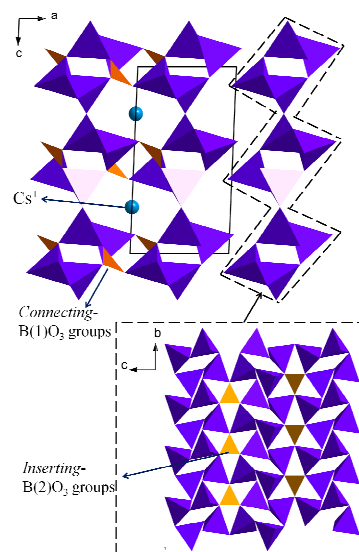
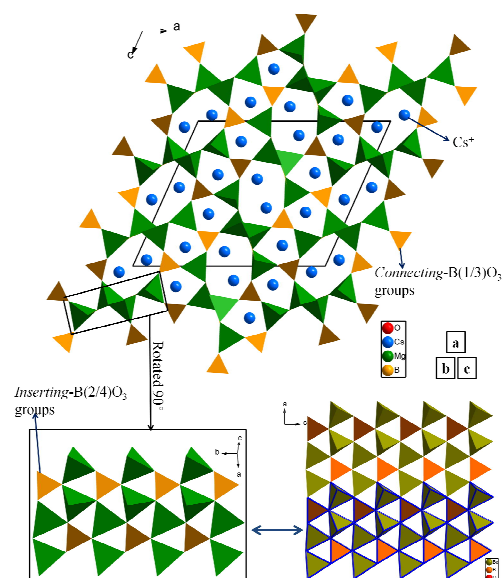


Figure 2. Structure of CZBO and 2D  $[\text{Zn}_4\text{O}_9]_\infty$  layers.

CMBO belongs to the space group  $P2_1/c$  (No. 14) the asymmetric unit consists of four unique cesium atom, four unique magnesium atom, four unique boron atom, and twelve unique oxygen atoms (Table S1 in the Supporting Information). In the structure, four kinds of  $\text{MgO}_4$  tetrahedra form a 1D  $[\text{Mg}_4\text{O}_{15}]_\infty$  infinite chain with  $\text{B(2)O}_3$  and  $\text{B(4)O}_3$  groups inserted in the interspaces, then 1D chains further connect to 3D framework by  $\text{B(1)O}_3$  and  $\text{B(3)O}_3$  groups and form two kinds of tunnels along  $b$  direction with  $\text{Cs}^+$  cations distributed in Figures 3a and 3b. The function of two kinds of  $\text{BO}_3$  groups in CMBO is similar to that of CZBO (Figure S2c in the Supporting Information). The Mg-O distances are in the range  $1.871(7)$ – $1.995(4)$  Å and with an average bond distance of  $1.945$  Å which is shorter than that of RMBO, and B-O bond lengths range from  $1.345(8)$  to  $1.412(10)$  Å (an average distance of  $1.375$  Å). All four kinds of  $\text{Cs}^+$  cations bond with nine oxygen atoms with Cs-O bond distances in the range  $3.000(5)$ – $3.723(4)$  Å (an average distance of  $3.379$  Å). BVS calculation (Cs  $0.91$ – $1.02$ , Mg  $2.01$ – $2.06$ , B  $2.92$ – $3.05$ , O  $1.91$ – $2.13$  (Table S1 in the Supporting Information)) indicates that bond valences are reasonable.



**Figure 3.** (a) Structure of CMBO; (b) 1D Mg-B-O chain of CMBO; (c) the  $[\text{Be}_2\text{BO}_5]_\infty$  2D layer of  $\beta$ -,  $\gamma$ - $\text{KBe}_2\text{B}_3\text{O}_7$  and  $\text{RbBe}_2\text{B}_3\text{O}_7$  (in order to identify, similar segment is highlighted).

Interestingly, the topological structure of 1D chain in CMBO is similar to that of  $\text{Li}_{0.8}\text{Mg}_{2.1}\text{B}_2\text{O}_5\text{F}^{23}$  which was reported by our group, except for the angles of adjacent chains in CMBO is about  $90^\circ$  and that of  $\text{Li}_{0.8}\text{Mg}_{2.1}\text{B}_2\text{O}_5\text{F}$  is about  $51^\circ$  (Figure S3 in the Supporting Information). The 1D cationic chain of two compounds attribute for their needlelike crystal morphology (Figure S4 in the Supporting Information). In addition, the connection mode of  $\text{MgO}_4$  tetrahedra and  $\text{BO}_3$  groups in CMBO is similar to that of the segment of  $[\text{Be}_2\text{BO}_5]_\infty$  layers in  $\beta$ -,  $\gamma$ - $\text{KBe}_2\text{B}_3\text{O}_7$  and  $\text{RbBe}_2\text{B}_3\text{O}_7$ ,<sup>24</sup> which is highlighted in Figure 3c. So it is a possible way to synthesize new compound via the replacement of beryllium in the beryllium borates with nontoxic magnesium.

In addition, the first title compound RMBO is isostructural with  $\text{KMgBO}_3$  (KMBO) reported by Wu et al.<sup>25</sup> According to the similar chemical properties and cationic radius, the isostructural  $\text{CsMgBO}_3$  may exist, but we failed to obtain it. While the title compound CMBO is a new structure with same elements ratio to RMBO and KMBO. Owing to the different interaction of Mg-O cationic skeletons on the arrangement of  $\text{BO}_3$  triangles, the isolated  $\text{BO}_3$  groups in RMBO arrange around crystallographic  $a$ ,  $b$  and  $c$  axis in an axial  $\text{C}_2$  symmetry and around four body diagonals in an axial  $\text{C}_3$  symmetry (Figure S5a), following the symmetry operation of the point group  $23$ , which allows RMBO

to crystallize in noncentrosymmetric space group. While the isolated  $\text{BO}_3$  groups of CMBO arrange in an inversion centre symmetry and in a mirror symmetry perpendicular to  $[010]$  direction and around  $b$  axis in an axial  $\text{C}_2$  symmetry (Figure S5b), following the symmetry operation of the point group  $\text{C}_{2h}$ , which lead to a centrosymmetric structure.

### The Influence of Cationic Skeleton on the Arrangement of Isolated $\text{BO}_3$ Groups

In the three borates that only containing isolated  $\text{BO}_3$  groups, the cationic skeleton formed by small cations ( $\text{Mg}^{2+}$  and  $\text{Zn}^{2+}$ ) with strong bonding are beneficial to form isolated  $\text{BO}_3$  groups rather than B-O network, which means that the arrangements of isolated  $\text{BO}_3$  groups are significantly influenced by the Mg-O or Zn-O skeletons. Based on the cationic skeleton structures of three compounds, it is reasonable to understand that how the arrangement of isolated  $\text{BO}_3$  groups are influenced by the cationic skeletons. The 3D skeleton of RMBO has more constraints to limit the orientation of isolated  $\text{BO}_3$  groups, so it is difficult to obtain the parallel  $\text{BO}_3$  groups (Figure 4a). While 2D (CZBO) and 1D (CMBO) skeletons reduce a dimensional constraint, so it is possible to obtain the parallel  $\text{BO}_3$  groups (Figures 4b and 4c). Hence, lower-dimensional skeletons are beneficial to obtain parallel  $\text{BO}_3$  groups. Recently, using of lower-dimensional skeletons controlling the isolated  $\text{BO}_3$  groups to arrange parallelly to obtain excellent properties also can be seen in birefringent crystals ( $\text{NaMgBO}_3$ <sup>26</sup>), KBBF ( $\text{KBe}_2\text{BO}_3\text{F}_2$ )<sup>27</sup> series nonlinear optical crystals and fluorescent materials (such as:  $\text{KMgBO}_3$ <sup>25</sup>,  $\text{Ba}_2\text{Mg}(\text{BO}_3)_2$ <sup>28</sup>).

### 60 Thermal Analysis

Viewing from the TG-DSC curves of RMBO, CZBO and CMBO (Figure 5), all of three compounds only appear one clear endothermic peak at  $865$ ,  $993$  and  $761^\circ\text{C}$ , respectively, and corresponding with obvious weight loss, which tentatively suggests that the three compounds melt incongruently. In order to assign the endothermic peak, the samples of three compounds were calcined at  $900$ ,  $1050$  and  $800^\circ\text{C}$  for 10 h, respectively. As shown in Figure S1, RMBO and CMBO are decomposed into  $\text{Mg}_3(\text{BO}_3)_2$  (JCPDS No. 38-1475), and  $\text{MgO}$  (JCPDS No. 04-0829) with the volatilization of Rb and Cs elements; CZBO is decomposed into  $\text{Zn}_3(\text{BO}_3)_2$  (JCPDS No. 27-0983) and partial unknown phases with the volatilization of Cs element. Hence, the three endothermic peaks are the decomposed peaks of RMBO, CZBO and CMBO compounds, and the flux should be introduced to decrease the crystal growth temperature.

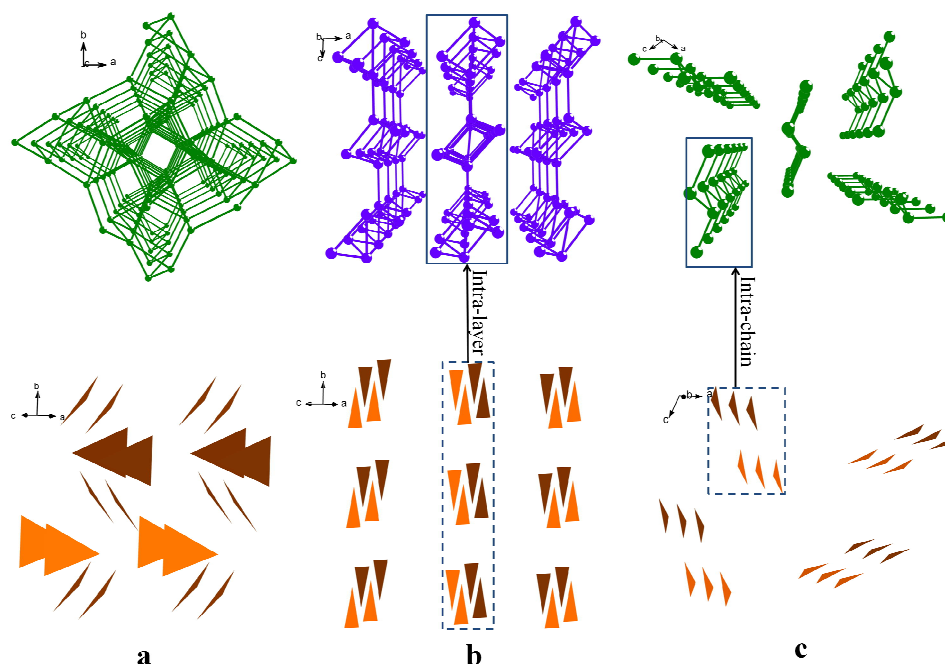


**Figure 4.** The Mg and Zn cationic skeletons of (a) RMBO, (b) CZBO and (c) CMBO, and the arrangements of  $\text{BO}_3$  groups of RMBO, intra-layer  $\text{BO}_3$  groups of CZBO and intra-chain  $\text{BO}_3$  groups of CMBO (oxygens are omitted and cations shared oxygens are bonded for clarity).

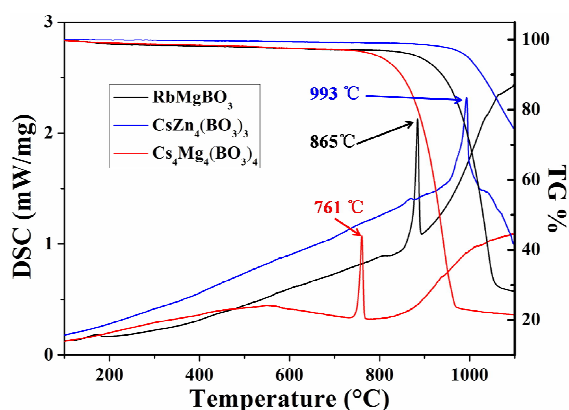


**Figure 5.** TG-DSC curves of (a) RMBO, (b) CZBO and (c) CMBO.

### Linear Optical Properties Characterization

Figure S6 in the Supporting Information shows the UV-Vis-NIR diffuse reflectance spectra of RMBO, CZBO and CMBO. To determine the band gap being direct or indirect, the plots of  $(\alpha h\nu)^2$  and  $(\alpha h\nu)^{1/2}$  versus  $h\nu$  were performed.<sup>29</sup> In RMBO and CMBO, the band gaps obtained from the plots of  $(\alpha h\nu)^2$  versus  $h\nu$  are consistent with the color of the compounds, while the band gaps obtained from the plots of  $(\alpha h\nu)^{1/2}$  versus  $h\nu$  is consistent with the color of CZBO. Actually, the power samples of three compounds are all white. So RMBO and CMBO should be direct band structure with band gaps of 4.76 and 5.39 eV, respectively, and CZBO is indirect band structure with band gap of 5.18 eV.

### Electronic Band Structures

Electronic structure calculations were performed in order to examine their band structures and explain the relationships

between electronic structures and optical properties. The electronic band structures of RMBO, CZBO and CMBO were determined using the plane-wave pseudopotential calculations. The calculated band structures of RMBO, CZBO and CMBO along high symmetry points of the first Brillouin zone are plotted in Figure 6. It is found that the lowest energy of the conduction bands (CBs) is localized at the G, B and D point for three compounds, respectively, whereas the highest of the valence bands (VBs) is localized at the G point with a band gap of 4.55 for RMBO, at the D point with a band gap of 4.50 eV for CMBO, and at the A point with a band gap of 4.23 eV for CZBO. Therefore, RMBO and CMBO are direct bandgap insulators and CZBO is indirect bandgap insulator. The calculated band gaps of the three compounds are smaller than the experimental band gaps.

As seen from the total and partial densities of states (TDOS, PDOS) analyses (Figure 6), the VBs below the Fermi level are mainly derived from Mg 2*p* and 3*s* orbitals and O 2*p* orbitals for RMBO; CZBO are mainly derived from Zn 3*d* orbitals and O 2*p* orbitals; and that of CMBO are mainly derived from O 2*p* orbitals. While, for RMBO, the CBs above the Fermi level are mainly derived from Rb 4*p* and 5*s* orbitals and B 2*p* orbitals; for CZBO, that are mainly derived from Cs 5*p* and 6*s* orbitals and Zn 3*p* and 4*s* orbitals and B 2*p* orbitals and O 2*p* orbitals; CMBO are mainly derived from Cs 5*p* and 6*s* orbitals and Mg 2*p* orbitals and B 2*s* and 2*p* orbitals and O 2*p* orbitals. One can see that the band gaps for RMBO and CMBO are mainly determined by charge transfers from Mg-O, whereas Zn-O decides that of CZBO which indicates a relatively smaller band gap.

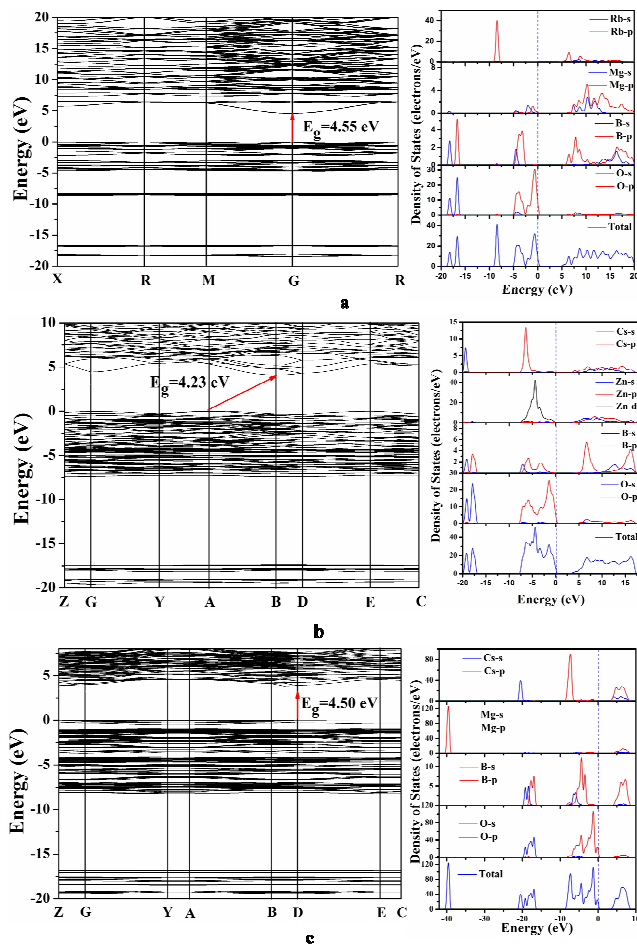


**Figure 6.** Band structures, Total DOS and partial DOS of (a) RMBO, (b) CZBO and (c) CMBO.

## Conclusions

Three borates,  $\text{RbMgBO}_3$ ,  $\text{CsZn}_4(\text{BO}_3)_3$  and  $\text{Cs}_4\text{Mg}_4(\text{BO}_3)_4$ , were reported and enrich the borate chemistry. The anionic groups of three compounds are isolated  $\text{BO}_3$  groups because the  $\text{Mg}^{2+}$  and  $\text{Zn}^{2+}$  cations in three compounds strongly bond with  $\text{O}^{2-}$  and preventing the polymerization of B and O. Different skeletons play different roles in the arrangement of isolated  $\text{BO}_3$  groups: the structure of  $\text{RbMgBO}_3$  presents 3D  $[\text{MgO}_3]_\infty$  framework which leads to  $\text{BO}_3$  groups distribute in the voids; the 2D  $[\text{Zn}_4\text{O}_9]_\infty$  layered structure of  $\text{CsZn}_4(\text{BO}_3)_3$  result in intra-layer  $\text{BO}_3$  groups parallel arrangement;  $\text{Cs}_4\text{Mg}_4(\text{BO}_3)_4$  features a 1D  $[\text{Mg}_4\text{O}_{15}]_\infty$  infinite chain which leads to the parallel arrangement of intra-chain  $\text{BO}_3$  groups. Further investigation for the influence of cation on the arrangement of isolated  $\text{BO}_3$  groups is underway.

## Acknowledgments

This work is supported by Western Light of CAS (Grant No. XBBS201217), 973 Program of China (Grant No. 2012CB626803), the National Natural Science Foundation of China (Grant Nos. U1129301, 51172277, 21101168, 11104344), Main Direction Program of Knowledge Innovation of CAS (Grant No. KJCX2-EW-H03-03), The Funds for Creative Cross

& Cooperation Teams of CAS, Major Program of Xinjiang Uygur Autonomous Region of China during the 12th Five-Year Plan Period (Grant No. 201130111), the High Technology Research & Development Program of Xinjiang Uygur Autonomous Region of China (Grant No. 201116143), the Science and Technology Project of Urumqi (Grant No. G121130002).

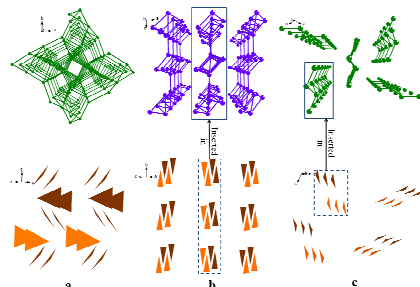
## Notes and references

- <sup>a</sup> Key Laboratory of Functional Materials and Devices for Special Environments of CAS, Xinjiang Technical Institute of Physics & Chemistry of CAS, Xinjiang Key Laboratory of Electronic Information Materials and Devices, 40-1 South Beijing Road, 830011 Urumqi, (P.R. China) Fax: (+86)991-3838957  
<sup>b</sup> University of Chinese Academy of Sciences, 100049 Beijing, (P.R. China)  
 † Electronic Supplementary Information available: [Table with atomic coordinates, equivalent isotropic displacement parameters, and selected bond lengths. XRD patterns, the ORTEP figure, the angles of adjacent chains in CMBO and  $\text{Li}_{0.8}\text{Mg}_{2.1}\text{B}_2\text{O}_5\text{F}$ , crystals picture of CMBO, the orientation of isolated  $\text{BO}_3$  groups in RMBO and CMBO, UV-Vis-NIR diffuse reflectance spectra, Oscilloscope traces of the SHG signals of KDP and RMBO powder]. See DOI: 10.1039/b000000x/  
 ‡ the CCDC numbers:  $\text{Cs}_4\text{Mg}_4(\text{BO}_3)_4$  (991317);  $\text{CsZn}_4(\text{BO}_3)_3$  (991318)  $\text{RbMgBO}_3$  (991319).
- (a) P. Becker, *Adv. Mater.* 1998, **10**, 979; (b) P. S. Halasyamani and K. R. Poeppelmeier, *Chem. Mater.* 1998, **10**, 2753; (c) J. D. Grice, P. C. Burns and F. C. Hawthorne, *Can. Mineral.* 1999, **37**, 731; (d) T. Sasaki, Y. Mori, M. Yoshimura, Y. K. Yap and T. Kamimura, *Mater. Sci. Eng.* 2000, **R 30**, 1; (e) S. L. Pan, Y. C. Wu, P. Z. Fu, G. C. Zhang, Z. H. Li, C. X. Du and C. T. Chen, *Chem. Mater.* 2003, **15**, 2218; (f) C. Chen, Z. Lin and Z. Wang, *Appl. Phys. B* 2005, **80**, 1.
  - (a) C. T. Chen, N. Ye, J. Lin, J. Jiang, W. Zeng and B. Wu, *Adv. Mater.* 1999, **11**, 1071; (b) F. Li, S. L. Pan, X. L. Hou and J. Yao, *Cryst. Growth Des.* 2009, **9**, 4091; (c) X. Y. Fan, S. L. Pan, X. L. Hou, X. L. Tian and J. Han, *Cryst. Growth Des.* 2010, **10**, 252.
  - C. T. Chen and G. Z. Liu, *Ann. Rev. Mater. Sci.* 1986, **16**, 203.
  - (a) C. T. Chen, G. L. Wang, X. Y. Wang and Z. Y. Xu, *Appl. Phys. B* 2009, **97**, 9; (b) R. K. Li and Y. Y. Ma, *CrystEngComm* 2012, **14**, 5421; (c) P. Minzioni, G. Nava, I. Cristiani, W. Yan and V. Degiorgio, *Opt. Laser. Technol.* 2013, **50**, 71; (d) L. Wu, X. L. Chen, Y. Zhang, Y. F. Kong, J. J. Xu and Y. P. Xu, *J. Solid State Chem.* 2006, **179**, 1219; (e) H. W. Yu, H. P. Wu, S. L. Pan, Y. Wang, Z. H. Yang and X. Su, *Inorg. Chem.* 2013, **52**, 5359; (f) H. W. Yu, S. L. Pan, H. P. Wu, W. W. Zhao, F. F. Zhang, H. Y. Li and Z. H. Yang, *J. Mater. Chem.* 2012, **22**, 2105.
  - P. Becker, *Z. Kristallogr.* 2001, **216**, 523.
  - R. Gautier and K. R. Poeppelmeier, *Cryst. Growth Des.* 2013, **13**, 4084.
  - R. K. Li and P. Chen, *Inorg. Chem.* 2010, **49**, 1561.
  - (a) G. D. Chryssikos, E. I. Kamitsos and M. A. Karakassides, *Phys. Chem. Glasses* 1990, **31**, 109; (b) G. D. Chryssikos, E. I. Kamitsos, A. P. Patsis and M. A. Karakassides, *Mater. Sci. Eng. B* 1990, **7**, 1; (c) E. I. Kamitsos, *J. Phys. IV*, 1992, **2**, C2-87; (d) H. P. Wu, H. W. Yu, Z. H. Yang, X. L. Hou, X. Su, S. L. Pan, K. R. Poeppelmeier and J. M. Rondinelli, *J. Am. Chem. Soc.* 2013, **135**, 4215; (e) Y. Yang, S. L. Pan, J. Han, X. L. Hou, Z. X. Zhou, W. W. Zhao, Z. H. Chen and M. Zhang, *Cryst. Growth Des.* 2011, **11**, 3912; (f) Y. Yang, S. L. Pan, X. L. Hou, X. Y. Dong, X. Su, Z. H. Yang, M. Zhang, W. W. Zhao and Z. H. Chen, *CrystEngComm* 2012, **14**, 6720; (g) H. W. Yu, H. P. Wu, S. L. Pan, Z. H. Yang, X. Su and F. F. Zhang, *J. Mater. Chem.* 2012, **22**, 9665; (h) F. Kong, S. P. Huang, Z. M. Sun, J. G. Mao and W. D. Cheng, *J. Am. Chem. Soc.* 2006, **128**, 7750; (i) W. J. Yao, H. W. Huang, J. Y. Yao, T. Xu, X. X. Jiang, Z. S. Lin and C. T. Chen, *Inorg. Chem.* 2013, **52**, 6136.

- 9 (a) H. W. Huang, J. Y. Yao, Z. S. Lin, X. Y. Wang, R. He, W. J. Yao, N. X. Zhai and C. T. Chen, *Angew. Chem. Int. Ed.* 2011, **50**, 9141; (b) T. K. Bera, J. H. Song, A. J. Freeman, J. I. Jang, J. B. Ketterson and M. G. Kanatzidis, *Angew. Chem. Int. Ed.* 2008, **120**, 7946; (c) T. K. Bera, J. H. Song, A. J. Freeman, J. I. Jang, J. B. Ketterson and M. G. Kanatzidis, *Angew. Chem. Int. Ed.* 2008, **47**, 7828; (d) T. K. Bera, J. I. Jang, J. B. Ketterson and M. G. Kanatzidis, *J. Am. Chem. Soc.* 2009, **131**, 75; (e) M. R. Marvel, J. Lesage, J. Baek, P. S. Halasyamani, C. L. Stern and K. R. Poeppelmeier, *J. Am. Chem. Soc.* 2007, **129**, 13963.
- 10 (a) R. V. Kurbatov, L. A. Solovyov, B. G. Bazarov, A. K. Subanakov and J. G. Bazarova, *Solid State Commun.* 2013, **172**, 33; (b) R. W. Smith, J. L. Luce and D. A. Keszler, *Inorg. Chem.* 1992, **31**, 4679.
- 11 SAINT: Program for Area Detector Absorption Correction, Version 4.05; Siemens Analytical X-ray Instruments: Madison, WI, 1995.
- 12 R. H. Blessing, *Acta Crystallogr. Sect. A* 1995, **51**, 33.
- 13 G. M. Sheldrick, *SHELXTL, version 6.12*, Bruker Analytical X-ray Instruments, Inc.: Madison, WI, 2001.
- 14 G. M. Sheldrick, *SHELXS-97, Program for X-ray Crystal Structure Solution*, University of Göttingen, Göttingen, Germany, 1997.
- 15 L. J. Spek, *Appl. Crystallogr.* 2003, **36**, 7.
- 16 (a) P. Kubelka and F. Z. Munk, *Tech. Phys.* 1931, **12**, 593; (b) J. Tauc, *Mater. Res. Bull.* 1970, **5**, 721.
- 17 (a) M. D. Segall, P. J. D. Lindan, M. J. Probert, C. J. Pickard, P. J. Hasnip, S. J. Clark and M. C. Payne, *J. Phys.: Condens. Matter* 2002, **14**, 2717; (b) V. Milman, B. Winkler, J. A. White, C. J. Pickard, M. C. Payne, E. V. Akhmatkaya and R. H. Nobes, *Int. J. Quantum Chem.* 2000, **77**, 895.
- 18 J. P. Perdew, K. Burke and M. Ernzerhof, *Phys. Rev. Lett.* 1996, **77**, 3865.
- 19 J. S. Lin, A. Qteish, M. C. Payne and V. Heine, *Phys. Rev. B* 1993, **47**, 4174.
- 20 L. Wu, X. L. Chen, Y. P. Xu and Y. P. Sun, *Inorg. Chem.* 2006, **45**, 3042.
- 21 (a) Y. Wang, S. L. Pan, X. Su, Z. H. Yang, L. Y. Dong and M. Zhang, *Inorg. Chem.* 2013, **52**, 1488; (b) X. A. Chen, M. Li, J. L. Zuo, X. A. Chang, H. G. Zang and W. Q. Xiao, *Solid State Sci.* 2007, **9**, 678.
- 22 (a) I. D. Brown and D. Altermatt, *Acta Crystallogr. Sect. B* 1985, **41**, 244; (b) N. E. Brese and M. O'Keeffe, *Acta Crystallogr. Sect. B* 1991, **47**, 192.
- 23 Z. Wang, M. Zhang, S. L. Pan, Y. Wang, H. Zhang and Z. H. Chen, *Dalton Trans.* 2014, **43**, 2828.
- 24 S. C. Wang, N. Ye, W. Li and D. Zhao, *J. Am. Chem. Soc.* 2010, **132**, 8779.
- 25 L. Wu, J. C. Sun, Y. Zhang, S. F. Jin, Y. F. Kong and J. J. Xu, *Inorg. Chem.* 2010, **49**, 2715.
- 26 L. Wu, Y. Zhang, Y. F. Kong, T. Q. Sun, J. J. Xu and X. L. Chen, *Inorg. Chem.*, 2007, **46**, 5207.
- 27 L. Mei, X. Huang, Y. Wang, Q. Wu, B. C. Wu and C. T. Chen, *kristallogr.* 1995, **210**, 93.
- 28 H. H. Lin, H. B. Liang, G. B. Zhang and Q. Su, *Appl. Phys. A*, 2011, **105**, 143.
- 29 (a) T. H. Bang, S. H. Choe, B. N. Park, M. S. Jin and W. T. Kim, *Semicond. Sci. Technol.* 1996, **11**, 1159; (b) K. Mitchell, F. Q. Huang, A. D. McFarland, C. L. Haynes, R. C. Somers, R. P. Van Duyne and J. A. Ibers, *Inorg. Chem.* 2003, **42**, 4109.

**Table of contents**

**Manuscript title:** Exploring the influence of cationic skeletons on the arrangement of isolated  $\text{BO}_3$  groups based on  $\text{RbMgBO}_3$ ,  $\text{CsZn}_4(\text{BO}_3)_3$  and  $\text{Cs}_4\text{Mg}_4(\text{BO}_3)_4$ .



Cationic skeletons formed by cations with strong bonding ( $\text{Mg}^{2+}$  and  $\text{Zn}^{2+}$ ) can influence the arrangement of isolated  $\text{BO}_3$  groups, and lower-dimensional cationic skeletons are beneficial to obtain arranged  $\text{BO}_3$  groups.